

Intensity correlation properties of x-ray beams split with Laue diffraction

Chang-Zhe Zhao(赵昌哲), Shang-Yu Si(司尚禹), Hai-Peng Zhang(张海鹏), Lian Xue(薛莲), Zhong-Liang Li(李中亮), and Ti-Qiao Xiao(肖体乔)

Citation: Chin. Phys. B, 2024, 33 (**1**): 014102. DOI: 10.1088/1674-1056/acf206

Journal homepage: http://cpb.iphy.ac.cn; http://iopscience.iop.org/cpb

What follows is a list of articles you may be interested in

Investigations of moiré artifacts induced by flux fluctuations in x-ray dark-field imaging

Zhi-Li Wang(王志立), Zi-Han Chen(陈子涵), Yao Gu(顾瑶), Heng Chen(陈恒), and Xin Ge(葛昕)

Chin. Phys. B, 2023, 32 (**3**): 038704. DOI: 10.1088/1674-1056/ac946a

Analysis of refraction and scattering image artefacts in x-ray analyzer-based imaging

Li-Ming Zhao(赵立明), Tian-Xiang Wang(王天祥), Run-Kang Ma(马润康), Yao Gu(顾瑶), Meng-Si Luo(罗梦丝), Heng Chen(陈恒), Zhi-Li Wang(王志立), and Xin Ge(葛昕)

Chin. Phys. B, 2023, 32 (**2**): 028701. DOI: 10.1088/1674-1056/ac685d

X-ray phase-sensitive microscope imaging with a grating interferometer: Theory and simulation

Jiecheng Yang(杨杰成), Peiping Zhu(朱佩平), Dong Liang(梁栋), Hairong Zheng(郑海荣), and Yongshuai Ge(葛永帅)

Chin. Phys. B, 2022, 31 (**9**): 098702. DOI: 10.1088/1674-1056/ac600e

Property of slice square polycapillary x-ray optics

Shi-Qi Peng(彭诗棋), Zhi-Guo Liu(刘志国), Tian-Xi Sun(孙天希), Kai Wang(王锴), Long-Tao Yi(易龙涛), Kui Yang(杨魁), Man Chen(陈曼), Jin-Bang Wang(王金榜)

Chin. Phys. B, 2016, 25 (**2**): 024102. DOI: 10.1088/1674-1056/25/2/024102

Polycapillary X-ray lens for secondary focusing Beijing synchrotron radiation source

Li Yu-De (李玉德), Lin Xiao-Yan (林晓燕), Liu Shi-Gang (刘世岗), He Jin-Long (何金龙), Guo Fei (郭非), Sun Tian-Xi (孙天希), Liu Peng (刘鹏)

Chin. Phys. B, 2013, 22 (**4**): 044103. DOI: 10.1088/1674-1056/22/4/044103

Intensity correlation properties of x-ray beams split with Laue diffraction

Chang-Zhe Zhao(赵昌哲)[1,2,3], Shang-Yu Si(司尚禹)[1,2,3], Hai-Peng Zhang(张海鹏)[3], Lian Xue(薛莲)[3], Zhong-Liang Li(李中亮)[1,2,3,†], and Ti-Qiao Xiao(肖体乔)[1,2,3,‡]

[1] *Shanghai Institute of Applied Physics, Chinese Academy of Sciences, Shanghai* 201800, *China*
[2] *University of Chinese Academy of Sciences, Beijing* 100049, *China*
[3] *Shanghai Synchrotron Radiation Facility, Shanghai Advanced Research Institute, Chinese Academy of Sciences, Shanghai* 201204, *China*

(Received 27 June 2023; revised manuscript received 1 August 2023; accepted manuscript online 21 August 2023)

Beam splitting is one of the main approaches to achieving x-ray ghost imaging, and the intensity correlation between diffraction beam and transmission beam will directly affect the imaging quality. In this paper, we investigate the intensity correlation between the split x-ray beams by Laue diffraction of stress-free crystal. The analysis based on the dynamical theory of x-ray diffraction indicates that the spatial resolution of diffraction image and transmission image are reduced due to the position shift of the exit beam. In the experimental setup, a stress-free crystal with a thickness of hundred-micrometers-level is used for beam splitting. The crystal is in a non-dispersive configuration equipped with a double-crystal monochromator to ensure that the dimension of the diffraction beam and transmission beam are consistent. A correlation coefficient of 0.92 is achieved experimentally and the high signal-to-noise ratio of the x-ray ghost imaging is anticipated. Results of this paper demonstrate that the developed beam splitter of Laue crystal has the potential in the efficient data acquisition of x-ray ghost imaging.

Keywords: x-ray ghost imaging, beam splitting with Laue diffraction, intensity correlation, dynamical theory of x-ray diffraction

PACS: 41.50.+h, 87.59.–e **DOI:** 10.1088/1674-1056/acf206

1. Introduction

The x-ray imaging techniques, such as x-ray computed microtomography, full-field microscopy, and lensless imaging techniques, have been advanced by the development of high-brightness and high-coherence x-ray sources.[1–3] However, those so-called local imaging methods cannot achieve high-resolution, large field of view, and low-dose x-ray imaging simultaneously. Therefore, the non-local imaging method of x-ray ghost imaging is proposed to breakthrough the inherent limitations of conventional imaging.[4–7] Ghost imaging, also known as quantum correlation imaging or intensity correlation imaging, divides the incident beam with spatial intensity fluctuations into two beams by a beam splitter. The bucket detector in the object arm collects the total intensity of photons passing through the sample meanwhile the modulated beam in the reference arm is recorded by a detector with spatial resolution. By correlating the information collected from both paths, the structural information of the sample can be reconstructed.[8–10] For the implementation of x-ray ghost imaging, the main obstacle lies in achieving efficient x-ray beam splitting, and several x-ray ghost imaging methods have been developed.[5,6,11]

At present, x-ray ghost imaging is predominantly implemented through three approaches. The first approach is computational ghost imaging, which employs a bucket detector to measure intensity with known mask modulation and enables the direct reconstructing of sample information.[11,12] However, this approach requires an accurately fabricated x-ray mask. The second approach based on a single x-ray beam captures object and reference information by moving the sample into and out of the beam mechanically. And the sample information is reconstructed via correlation calculations on two sets of the image sequences.[5,13] Nevertheless, this approach features low data acquisition efficiency, which affects the extended application of this method.[6] The third approach is that in the beam-splitting scheme, the high efficiency of image acquisition can be achieved by using two detectors to measure the intensity fluctuations simultaneously, which has the potential in developing the dynamic x-ray ghost imaging. Nonetheless, the diffraction of Laue crystal reduces the spatial correlation between the two split beams owing to the interaction of x ray with crystal, which results in the deterioration of image and cannot show any advantages of x-ray ghost imaging.[14–17] Therefore, further research is needed to improve the correlation of the split x-ray beams aiming at x-ray ghost imaging with efficient projection collection. During the experiments of x-ray beam splitting, the clamping stress and mechanical vibration of the Laue crystal cannot be ignored. To address

†Corresponding author. E-mail: lizhongliang@sari.ac.cn
‡Corresponding author. E-mail: tqxiao@sari.ac.cn

© 2024 Chinese Physical Society and IOP Publishing Ltd

these issues, we design a stress-free splitter with a vibration isolation base.

In addition, the interaction of x rays with the crystal is an essential factor that affects the intensity correlation between diffraction beam and transmission beam. According to the dynamical theory of x-ray diffraction, we investigate the factors that affect the intensity correlation between the two split beams. Stress-free crystals are processed for splitting the x-ray beam and the non-dispersive configuration is implemented to ensure the large imaging field for both diffraction beam and transmission beam. A strong correlation is achieved between the two beams due to a minor energy-flow shift of the exit beam. High-quality x-ray ghost imaging is anticipated with the strong correlation between the two split x-ray beams.

2. Theoretical analysis

The reconstructed image quality of ghost imaging is directly influenced by the correlation between the split beams,[18] and the resolution of the ghost imaging is determined by the point spread function of system, which can be expressed as the covariance of the intensity modulation.[15,19] To quantify the correlation between diffraction beam and transmission beam with spatial intensity distributions on the same scale, the two-dimensional Pearson correlation coefficient is employed in this study, which can evaluate the correlation and analyze the system resolution. In the work, we investigate the factors that affect the intensity correlation between diffraction beam and transmission beam and provides theoretical and experimental supports for beam splitting of strong correlation.

According to the different geometries, x-ray diffractions of crystal can be classified as Laue case and Bragg case.[20] In the Bragg case, the incident beam falls into the gap of the dispersion surface completely, resulting in total reflection and micrometer-level extinction distance within the crystal. Therefore, the crystal thickness should be smaller than extinction distance in total reflection region in order to achieve the beam splitting in the Bragg case. However, it poses great challenges to the processing of stress-free and defect-free crystals with micrometer-thick crystals. In the Laue case, the incident beam can penetrate the gap of the dispersion surface. And the intensity ratio of diffraction beam to transmission beams can be modulated quantitatively based on Pendellösung effect even if the crystal thickness is far more than the extinction distance.[21] Therefore, the paper opts for the Laue case to alleviate the difficulties associated with crystal fabrication.

Next, the factors that affect the correlation between diffraction and transmission beams will be analyzed based on the dynamical theory of x-ray diffraction. In a symmetric Laue case of no absorption, the angle between the direction of the energy flow and the lattice plane can be given by[22]

$$\Theta = \tan^{-1}\left[\left(\frac{-\eta^2+\eta\left(1+\eta^2\right)^{1/2}}{1+\eta^2-\eta\left(1+\eta^2\right)^{1/2}}\right)\tan\theta_{\mathrm{B}}\right], \tag{1}$$

where

$$\eta = \Delta\theta/\delta, \tag{2}$$

$$\delta = r_{\mathrm{e}}\lambda^2|P||F_h|/(\pi V\sin 2\theta_{\mathrm{B}}), \tag{3}$$

$$2d_{hkl}\sin\theta_{\mathrm{B}} = n\lambda. \tag{4}$$

In Eq. (1), η is the deviation parameter determined by the divergence angle of incident beam $\Delta\theta$ and the Darwin width 2δ of the crystal. In Eq. (3), $r_{\mathrm{e}} = 2.81794\times10^{-6}$ nm is the classical radius of electron, λ is the wavelength of the incident beam, P is the polarization factor, F_h is the crystal structure factor, V is the volume of the unit cell, and θ_{B} is the Bragg angle. Equation (4) is Bragg formula, where d_{hkl} is the space of lattice plane with index hkl. On the exit surface of the crystal, the position shift of the exit beam from the Bragg angle is given by

$$\Delta l = t\cdot|\tan\Theta|, \tag{5}$$

where t is the thickness of crystal. It can be demonstrated from Eq. (5) that the position shift of the exit beam leads to an anisotropic spatial resolution for diffraction beam and transmission beam in the diffraction direction,[23] which will reduce the resolution of the ghost imaging and the correlation of spatial intensity between the splitting beams.

In Laue case, the influence factors of the position shift of the exit beam are numerically calculated from Eqs. (1)–(5). Figure 1 shows $\Delta\theta$-dependence of the variations of position shift Δl with $\Delta\theta$ for different crystal thickness values and different indices of the lattice plane. In numerical analysis, the wavelength of the incident beam is set to 0.83 Å and the polarization direction of the x-ray beam is assumed to be perpendicular to the diffraction plane ($P = 1$). The solid line (red) represents the result of Si(111) diffraction with a 300-μm thickness crystal; the dashed line (black) represents the result of Si(111) diffraction with a 600-μm-thick crystal; the dotted line (green) represents the result of Si(220) diffraction with a 600-μm-thick crystal. In Fig. 1, on the one hand, the position shift of the exit beam increases sharply within a few arcseconds as the divergence angle of incident beam increases. On the other hand, higher indices of the lattice plane and larger thickness of the crystal cause a bigger position shift of the exit beam. At 15-keV photon energy, when the crystal thickness is 300 μm and divergence angle is 3.5″ which is the Darwin width of Si(111), the diffraction displacement of position shift of Si(111) can reach 28 μm. And the results (denoted with dots) are shown in Fig. 1. In such a condition, if the position shift of the exit beam is smaller than the smallest characteristic length scale of random illumination images in the ghost

imaging system,[24] the diffraction image and transmission image will have a strong correlation. According to the theoretical analysis, a thinner Laue crystal with lattice plane Si(111) should be the best option for the beam splitter in x-ray ghost imaging.

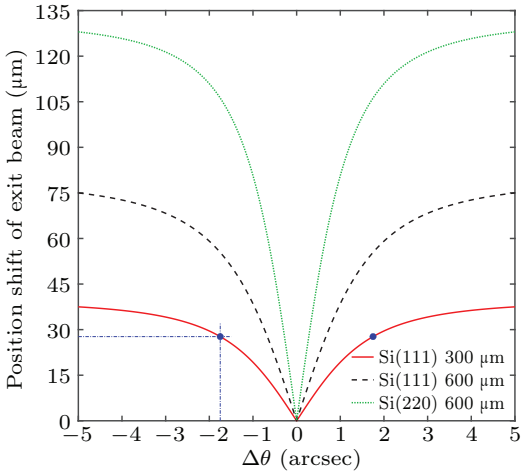


Fig. 1. Numerical results of position shift Δl varying with $\Delta\theta$ at different crystal thickness values and indices of lattice plane, with wavelength of incident beam being 0.83 Å and the polarization direction of x-ray beam being perpendicular to diffraction plane ($P = 1$).

3. Experiments

The experiments were conducted on the test beamline (BL09B) of Shanghai Synchrotron Radiation Facility (SSRF), which uses a bending magnet (BM) source with critical energy of 10 keV.[25]

As mentioned in the above section, a perfect thin crystal of stress-free is crucial for obtaining high-quality split beams. The design drawing of the beam splitter used in the experiment is shown in Fig. 2. A float-zone (FZ) monocrystalline silicon was processed through orientation, cutting, grinding, polishing and etching. Then perfect stress-free crystals with different thickness values could be obtained. Two orthogonal orientation of lattice plane (111) and $(1\bar{1}0)$ were selected as the surfaces of the crystal, which ensure that there are two sets of available lattice planes for diffraction in the same crystal. The crystal pedestal cutting from the same crystal was utilized for clamping during processing and experiment, which prevents the stress from spreading to the workspace of the splitter.

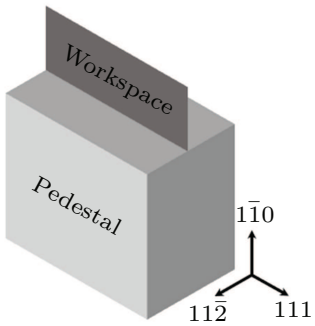


Fig. 2. Design drawing of beam-splitting crystal and crystal orientation.

Figure 3 is the optical layout of the beam splitting experiments, in which the photon energy of the x-ray beam was set to 15 keV by the rotating the Si(111) plane of the double-crystal monochromator (DCM). The distance between DCM and synchrotron radiation (SR) source was 21 m. The beam splitter was 18 m downstream from the DCM. The DCM and the beam splitter were arranged in a non-dispersive configuration in order to ensure sufficient imaging field for both diffraction beam and transmission beam. An ionization chamber (IC) was installed after the beryllium window to monitor the real-time beam intensity. A copper foam acting as a firm absorbing material provided a spatially random modulation of the beam intensity. Finally, a pixel array detector (OnSemi KAI-16000, CCD camera) was positioned 0.1 m behind the beam splitter to record diffraction image and transmission image simultaneously. The effective area of the detector is 36 mm×24 mm with a pixel size of 7.4 μm.

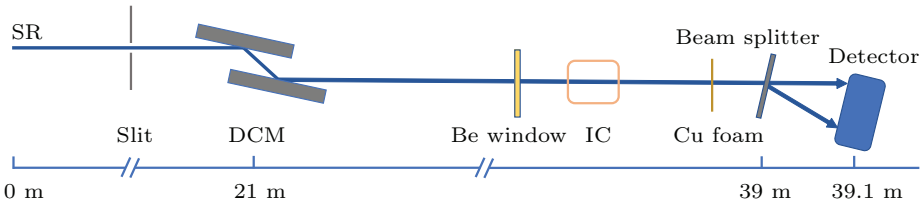


Fig. 3. Optical layout of beam splitting experiment.

4. Results and analyses

Two sets of images are obtained using the beam splitter with different thickness values and plane indices, which are shown in Fig. 4. Figures 4(a) and 4(b) are the results of a 300-μm-thick Si(111) crystal, which show a better spatial resolution. On the contrary, the hole structures are elongated and blurred in Figs. 4(c) and 4(d) where a 600-μm-thick Laue diffraction crystal is used, indicating that a thinner crystal can effectively alleviate the position shift of the exit beam. On the other hand, the high-index lattice planes are more susceptible to the divergence of the incident beam, which leads to severe blurring in the diffraction direction as shown in Figs. 4(e) and 4(f). Additionally, the "weak dispersion" configuration of the different lattice planes between DCM and the beam splitter

limits the imaging field of view.

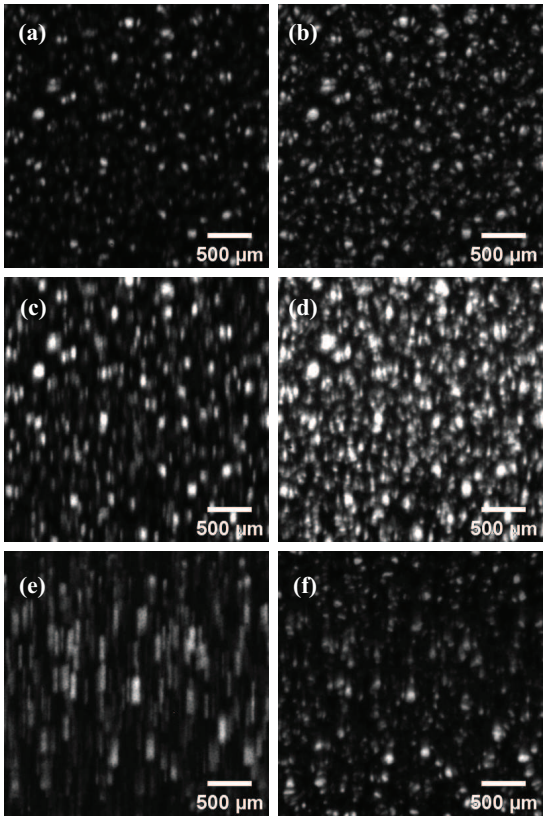


Fig. 4. Spatially random illumination diffraction (left) and transmission (right) images of beam splitting, showing the results of Si(111) diffraction of ((a), (b)) a 300-μm-thick crystal, ((c), (d)) a 600-μm-thick crystal, and ((e), (f)) of a 600-μm-thick Si(220) crystal.

To quantify the correlation between diffraction image and transmission image, the two-dimensional correlation coefficient is given by[26]

$$r(x-x',y-y') = \frac{[I_{\rm t}(x,y)-\overline{I_{\rm t}}][I_{\rm d}(x',y')-\overline{I_{\rm d}}]}{\sigma_{\rm t}(x,y)\sigma_{\rm d}(x',y')}, \tag{6}$$

where I is the gray value of the detected image at each pixel, (x,y) is the coordinate of each pixel, the subscripts d and t represent the diffracted beam and the forward diffracted beams respectively, I is the mean gray value of the image, and σ is the standard deviation of the gray value of the image. In the situation of adequate randomization of intensity modulation, the map of the two-dimensional correlation coefficient can be regarded as the point spread function of the ghost imaging system.[27] The maximum value of correlation map indicates the degree of linear correlation between diffraction image and transmission image, and the full width at half maximum (FWHM) of the peak provides the resolution information of the ghost imaging system.

The correlation maps calculated from diffraction image and transmission image in Fig. 4 are illustrated in Fig. 5. The vertical direction within the correlation maps aligns with the diffraction plane. As shown in Fig. 5(a), the correlation map exhibits strong correlation and approximately rotational symmetry for the beam splitter of 300-μm-thick crystal. However, figure 5(b) shows the broadening of the correlation map in the vertical direction, owing to the diffraction effect, which reduces the system resolution and the correlation between the two beams. Additionally, high-index crystal diffraction results in large loss of image information, leading to artifacts in the correlation map as observed in Fig. 5(c). Theoretically, the correlation maps generated from spatially random images should exhibit rotational symmetry. In experiment, the diffraction of the crystal affects the vertical direction more significantly than the horizontal direction.

To characterize the effects in the diffraction process, the correlation maps are further analyzed quantitatively as shown in Fig. 6. Figure 6(a) displays the central vertical profiles and figure 6(b) displays the central horizontal profiles. The line profiles reveal that the vertical widths are wider than the horizontal widths in each corresponding profile as shown in Fig. 6, which means that the dynamical effect has a larger influence in the diffraction plane. Furthermore, the horizontal resolution of ghost imaging is about 80 μm as shown in Fig. 6(b), which is dependent on the modulation of spatial intensity. And the vertical resolution of ghost imaging declines when the diffraction effect surpasses the intensity modulation. A maximum correlation coefficient of 0.92 can be achieved by the Si(111) Laue crystal with a thickness of 300 μm as shown in Fig. 6, which is quite close to the limitation predicted by the dynamical theory of crystal.

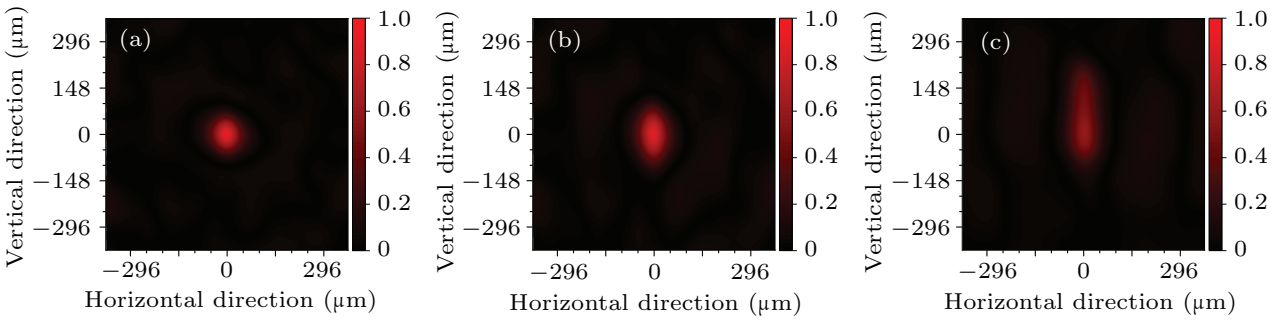


Fig. 5. Two-dimensional correlation coefficient maps of diffraction and transmission images. (a) Correlation map of the images in Figs. 4(a) and 4(b). (b) Correlation map of images in Figs. 4(c) and 4(d). (c) Correlation map of images in Figs. 4(e) and 4(f).

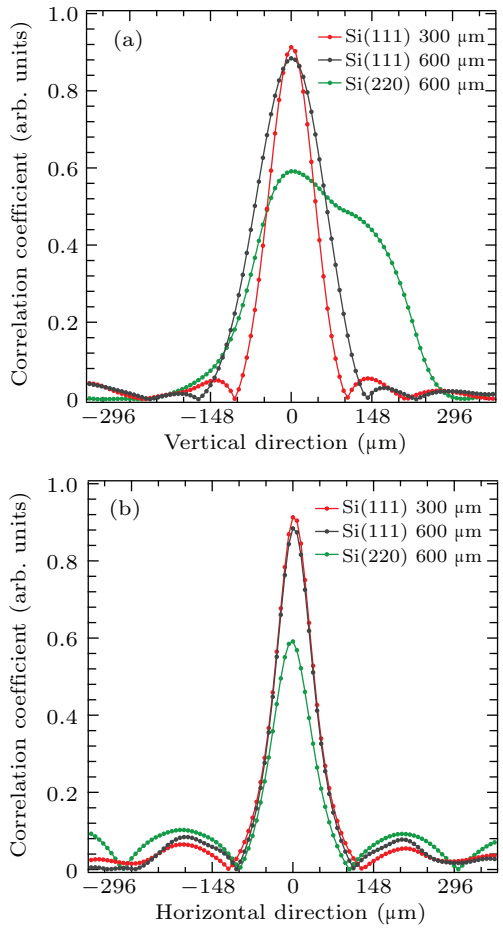


Fig. 6. Line profiles of two-dimensional correlation coefficient maps in Fig. 5. (a) Profiles in the central vertical direction. (b) Profiles in the central horizontal direction.

5. Conclusions

In this paper, we investigated the intensity correlation between diffraction beam and transmission beam based on the Laue diffraction of stress-free thin crystal. The theoretical analysis shows that the position shift of the exit beam leads to the reduction in the spatial resolution of both diffraction image and transmission image, in which the blurring is more pronounced in the diffraction direction. In experiment, a stress-free crystal with a thickness of hundred-micrometers-level is used for high-quality beam splitting, which is in a non-dispersive configuration equipped with the DCM to ensure the consistent size of the diffraction beam and the transmission beam. To quantify the correlation between diffraction beam and transmission beam with spatial intensity distributions on the same scale, the two-dimensional Pearson correlation coefficient is employed to evaluate the correlation properties and the spatial resolution of imaging system. A correlation coefficient of 0.92 is achieved and the high signal-to-noise ratio of the x-ray ghost imaging is anticipated. The research results of this work demonstrate that the developed beam splitter of Laue crystal may realize the efficient data acquisition of x-ray ghost imaging.

Acknowledgements

The authors thank Zhang X W, Diao Q S, and Hong Z for their fruitful discussion and kind help.

Project supported by the National Key Research and Development Program of China (Grant Nos. 2022YFF0709103, 2022YFA1603601, 2021YFF0601203, and 2021YFA1600703), the National Natural Science Foundation of China (Grant No. 81430087), and the Shanghai Pilot Program for Basic Research – Chinese Academy of Sciences, Shanghai Branch (Grant No. JCYJ-SHFY-2021-010).

References

[1] Eriksson M, Van der Veen J F and Quitmann C 2014 *J. Synchrotron Radiat.* **21** 837
[2] Emma P, Akre R, Arthur J, Bionta R, Bostedt C, Bozek J, Brachmann A, Bucksbaum P, Coffee R and Decker F J 2010 *Nat. Photon.* **4** 641
[3] Willmott P 2019 *An Introduction to Synchrotron Radiation: Techniques and Applications* (John Wiley and Sons) p. 367
[4] Cheng J and Han S S 2004 *Phys. Rev. Lett.* **92** 093903
[5] Yu H, Lu R H, Han S S, Xie H L, Du G H, Xiao T Q and Zhu D M 2016 *Phys. Rev. Lett.* **117** 113901
[6] Pelliccia D, Rack A, Scheel M, Cantelli V and Paganin D M 2016 *Phys. Rev. Lett.* **117** 113902
[7] Lane T J and Ratner D 2020 *Opt. Express* **28** 5898
[8] Klyshko D 1988 *Phys. Lett. A* **128** 133
[9] Bennink R S, Bentley S J and Boyd R W 2002 *Phys. Rev. Lett.* **89** 113601
[10] Zhang H P, Li K, Zhao C Z, Tang J and Xiao T Q 2022 *Chin. Phys. B* **31** 064202
[11] Klein Y, Schori A, Dolbnya I, Sawhney K and Shwartz S 2019 *Opt. Express* **27** 3284
[12] He Y H, Zhang A X, Li M F, Huang Y Y, Quan B G, Li D Z, Wu L A and Chen L M 2020 *APL Photon.* **5** 056102
[13] Zhang H P, Li K, Wang F X, Yu H, Zhao C Z, Du G H, Li Z L, Deng B, Xie H L, Han S S and Xiao T Q 2022 *Chin. Opt. Lett.* **20** 033401
[14] Schori A and Shwartz S 2017 *Opt. Express* **25** 14822
[15] Pelliccia D, Olbinado M P, Rack A, Kingston A M, Myers G R and Paganin D M 2018 *IUCrJ* **5** 428
[16] Kingston A M, Pelliccia D, Rack A, Olbinado M P, Cheng Y, Myers G R and Paganin D M 2018 *Optica* **5** 1516
[17] Zhang H P, Zhao C Z, Ju X L, Tang J and Xiao T Q 2022 *Acta Phys. Sin.* **71** 074201 (in Chinese)
[18] Liu H L, Shen X, Zhu D M and Han S S 2007 *Phys. Rev. A* **76** 053808
[19] Oh J E, Cho Y W, Scarcelli G and Kim Y H 2013 *Opt. Lett.* **38** 682
[20] Authier A 2010 *Dynamical theory of x-ray diffraction* (International Tables for Crystallography) pp. 626–646
[21] Zhao C Z, Si S Y, Zhang P H, Xue L, Li Z L and Xiao T Q 2022 *Acta Phys. Sin.* **71** 046101 (in Chinese)
[22] Kato N 1960 *Acta Crystallogr.* **13** 349
[23] Hirano K and Momose A 1999 *Jpn. J. Appl. Phys.* **38** L1556
[24] Oh J E, Cho Y W, Scarcelli G and Kim Y H 2013 *Opt. Lett.* **38** 682
[25] Li Z L, Fan Y C, Xue L, Zhang Z Y and Wang J 2019 *AIP Conference Proceedings*, June 10–15, 2019, Taiwan, China, p. 060040
[26] Ott R L and Longnecker M T 2015 *An Introduction to Statistical Methods and Data Analysis* (Cengage Learning) p. 587
[27] Ferri F, Magatti D, Lugiato L and Gatti A 2010 *Phys. Rev. Lett.* **104** 253603